Available online at www.sciencedirect.com
SCIENCE DIRECT
ELSEVIER
Coordination Chemistry Reviews 250 (2006) 1012–1022
COORDINATION CHEMISTRY REVIEWS
www.elsevier.com/locate/ccr

Review

Functionalized ferrocenes Unique properties based on electronic communication between amino group of the ligand and Fe center

Kohtaro Osakada *, Tatsuaki Sakano, Masaki Horie, Yuji Suzaki

Chemical Resources Laboratory, Tokyo Institute of Technology, 4259 Nagatduta, Midori-ku, Yokohama 226-8503, Japan

Received 25 August 2005; accepted 30 November 2005
Available online 30 January 2006

Contents

Abstract

Recent results of our studies on preparation and properties of the ferrocene derivatives with amine-containing ligands are reviewed. We established a route to 2-aza[3]ferrocenophanes with an *N*-aryl or *N*-alkyl substituent by using $RuCl_2(PPh_3)_3$ as catalyst for condensation of 1,1′-bis(hydroxymethyl)ferrocene with primary amines. The obtained ferrocenophanes show reversible redox of the Fe center. At higher potentials, quasi-reversible or irreversible electrochemical oxidation of amino groups of the ligand is observed for most of the 2-aza[3]ferrocenophanes. The initially formed one-electron-oxidized species undergo rapid and reversible intramolecular electron transfer between the Fe center and the nitrogen atom of the ligand. The 2-aza[3]ferrocenophanes with *N*-aryl group bonded to *trans*-aminoazobenzene group undergo photo-induced isomerization to its *cis* isomer, giving an equilibrated mixture under photostationary state. Electrochemical oxidation of the Fe(II) center shifts the equilibrium to formation of the *trans*-azobenzene even under photoirradiation. Thus, thermodynamics of the isomerization of azobenzene group is regulated by changing the oxidation state of the molecule. Protonation of ferrocene derivatives with aminomethyl group on the cyclopentadienyl ligand forms the dialkylammonium group which forms a complex with dibenzo[24]crown-8 (DB24C8) with interlocked structures. The pseudorotaxanes obtained were characterized by X-ray crystallography and mass spectrometry. Electrochemical oxidation of the ferrocene with aminomethyl group at a cyclopentadienyl ligand in the presence of 1-hydroxy-2,2,6,6-tetramethylpiperidine (TEMPOH) leads to formation of the dialkylammonium group which produces the pseudorotaxane instantly with added DB24C8.

Keywords: Ferrocene; Rotaxane; Azobenzene; Electrochemistry

1. Introduction

A number of the ferrocene derivatives have been synthesized and used as electronic and optical materials because the cyclopentadienyl (Cp) ligand of ferrocene is readily functionalized by nucleophilic organic reagents and because electrochemical properties of the $Fe(II)Cp_2$ fragment can be tuned by selecting the substituents introduced to the Cp ligand [1]. The redox between the neutral Fe(II) state and cationic Fe(III) state, involving fast and reversible electron transfer, is the important property of the ferrocene derivatives. Introduction of electrochemically active organic groups in the ligand of ferrocene forms the molecules containing the inorganic and organic redox-active centers. The ferrocene derivatives with aminoalkyl substituents at a Cp ligand were reported by Plenio et al. to show two electrochemical oxidation reactions, redox of the Fe center and

* Corresponding author. Tel.: +81 45 924 5224; fax: +81 45 924 5224.
E-mail address: kosakada@res.titech.ac.jp (K. Osakada).

0010-8545/$ – see front matter © 2005 Elsevier B.V. All rights reserved.
doi:10.1016/j.ccr.2005.11.022

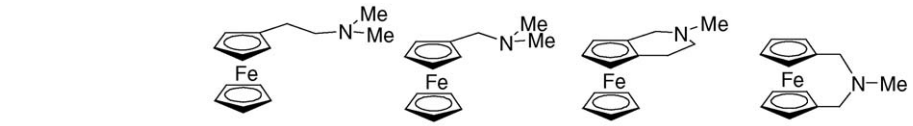

Fe-N distance (Å)	5.50	4.56	4.37	3.39
E_2 - E_1 (mV)	110	190	230	350

(E_1: redox potential of neutral compound; E_2: redox potential of the compound protonated at nitrogen)

Scheme 1.

oxidation of the amino group of the ligand [2]. The compounds having a shorter Fe–N distance exhibit a higher potential for oxidation of the amino group due to interaction between the Fe(III) center and the amino group (Scheme 1).

2-Aza[3]ferrocenophanes were reported to contain a short Fe–N distance due to the methylene spacer and to the cyclic structure that fixes relative positions of these atoms. Electron transfer between the Fe and N atoms of the 2-aza[3]ferrocenophanes is expected to take place easily.

Reports of detailed studies on the ferrocene derivatives with amino group in the ligand were limited partly because of lack in general preparation methods of these compounds. We have recently succeeded to prepare a series of the 2-aza[3]ferrocenophanes by using coupling reactions catalyzed by transition metal complexes and investigated detailed properties of these compounds. In this review article, we summarizes preparation, structures, and properties of the aminomethylferrocene and 2-aza[3]ferrocenophanes which function as unique materials responding to electrochemical stimulus.

2. Preparation and properties of 2-aza[3]ferrocenophanes

Murahashi, Tsuji, and their respective co-workers reported that $RuCl_2(PPh_3)_3$ catalyzed coupling of the compounds having OH and NH groups via condensation of these polar groups to form the products with new C–N bonds [3]. This type of reaction was employed for preparation of not only the organic compounds but also the polymers having polar functional groups [4]. We conducted condensation of 1,1′-bis(hydroxymethyl)ferrocene with primary amines catalyzed by the Ru complex and obtained 2-aza[3]ferrocenophanes, as shown in the following equation [5]:

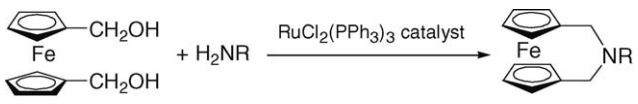

(1)

Chart 1 summarizes the ferrocenophanes prepared in this study. In spite of high temperature of the reaction (ca. 180 °C), cyclizative condensation of the diol with the aromatic and aliphatic amines produces the ferrocene derivatives whose cyclopentadienyl ligands are bridged by a CH_2–NR–CH_2 group in moderate and high yields.

Compounds **4**–**6**, **12**, and **15** having Br, OH, and ferrocenyl groups as the *N*-substituents are obtained selectively. Molecular structures of **1**–**3**, **8**, and **9** were determined by X-ray crystallography. The N–C bond distances are shown in Table 1. Compounds **1**–**3** have the N–C(aryl) bonds which are significantly shorter than the CH_2–N bond distance. It may be partly ascribed to an sp^2 character of the nitrogen atom bonded to the aromatic ring or possible canonical structures shown in Scheme 2.

The ferrocenophanes **11**, **13**, and **14** with *N*-alkyl substituent undergo addition of MeI to the nitrogen atom to form the ferrocenophane containing quaternary ammonium group and iodide as the counter anion **16**–**18**, as shown in Eq. (2). Exchange of the anion of **16** and **18** with BF_4^- leads to the formation of **19** and **20** smoothly:

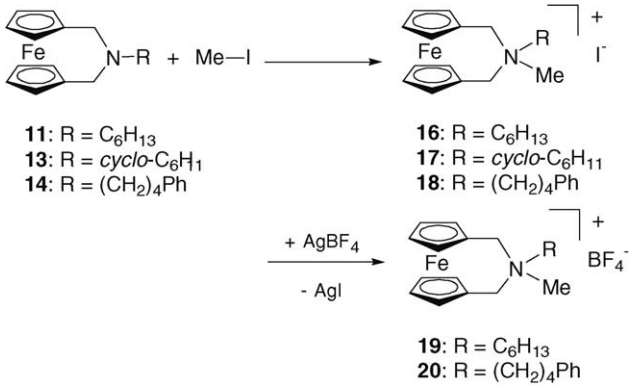

(2)

N–C bond distances of these ionic compounds (1.49–1.57 Å, Table 1) are in the range of C–N single bonds, and are consistent with the sp^3 hybridization of the nitrogen atom.

Cyclic voltammogram of the ferrocenophanes **1**–**14** in MeCN shows reversible electrochemical oxidation and reduction of the Fe center at $E_{1/2} = -0.02$ to $+0.08$ V (versus Ag^+/Ag), which are at similar positions to redox of ferrocene. Ferrocenophane **6** with 4-hydroxyphenyl group at the nitrogen atom shows additional reversible electrochemical oxidation and reduction at $E_{1/2} = +0.41$ V. Scheme 3 depicts the plausible mechanism that accounts for reversible two-step oxidation. Initial oxidation of **6** occurs at the Fe(II) center to form a ferrocenium species. Electron transfer from the amino group of the ligand to the Fe(III) center partly forms a Fe(II) species with radical cation at the

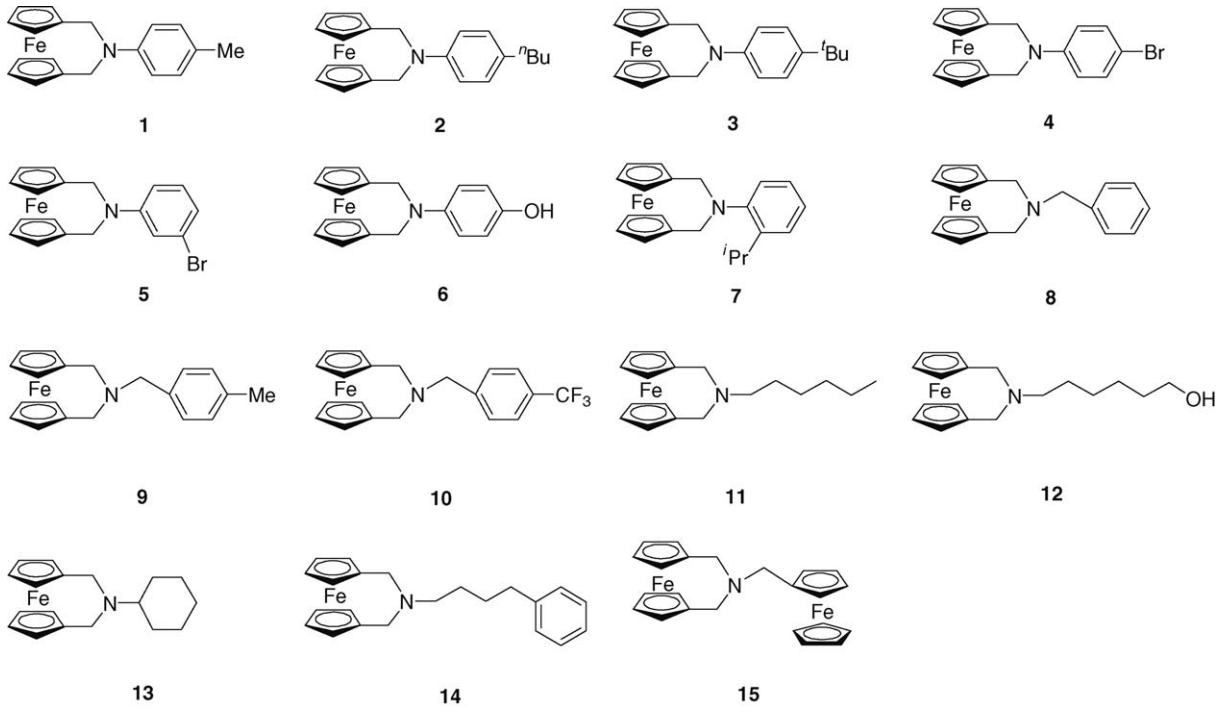

Chart 1.

nitrogen. The equilibrium between the two oxidized species is favored to formation of the ferrocenium. The radical cation species undergoes second electrochemical oxidation at the oxygen atom to yield the compound with cationic azaquinoid group which is stabilized by this π-conjugated structure.

Other 2-aza[3]ferrocenophanes with *N*-aryl substituent, **1**–**3** and **7**, exhibit reversible redox of the Fe center ($E_{1/2}$ = +0.04 to +0.08 V) and quasi-reversible or irreversible electrochemical oxidation at +0.67 to +0.72 V. The potential of the latter oxidation is higher than the corresponding potential of **6**. These elec-

Table 1
Bond parameters and electrochemical data of 2-aza[3]ferrocenophanes

Compound	Bond distance (Å)		CV data[a]		References
	CH_2–N	N–C(aryl)	1st[b]	2nd[c]	
1	1.48(1), 1.46(1)	1.37(1)	+0.08	+0.68	[5b]
2	1.467(6), 1.464(6)	1.400(6)	+0.08	+0.72	[5b]
3	1.44(1), 1.46(1)	1.38(1)	+0.06	+0.67	[5b]
6			−0.02	+0.41[b]	[5c]
7			+0.04	[d]	[5c]
8	1.460(5), 1.477(5)	1.472(4)[e]	+0.05	[d]	[5b]
9	1.466(8), 1.487(6)	1.463(7)[e]	+0.04	[d]	[5b]
10			+0.04	[d]	[5c]
11			+0.04	+0.35	[5b]
12			−0.01	+0.44 (E_{ox})[f]	[5c]
13			−0.01	+0.42 (E_{ox})[f]	[5c]
14			+0.04	+0.41 (E_{ox})[f]	[5c]
16	1.50(2), 1.55(2)	1.57(3), 1.49(3)[e]	+0.42		[5b,5c]
17	1.57(1), 1.54(1)	1.55(1), 1.50(1)[e]			[5c]
18			+0.37		[5c]
19	1.53(1), 1.56(1)	1.52(1), 1.52(1)[d]	+0.42		[5c]
20			+0.39		[5c]
Ferrocene			+0.04		[5b]

[a] Electrochemical potentials are obtained by cyclic voltammogram (CV) in MeCN containing $^nEt_4NBF_4$, used as the electrolyte. Potentials are referenced with Ag^+/Ag.
[b] Reversible.
[c] Quasi-reversible than otherwise stated.
[d] Not observed clearly.
[e] N–C(alkyl) bond distances are shown.
[f] Irreversible.

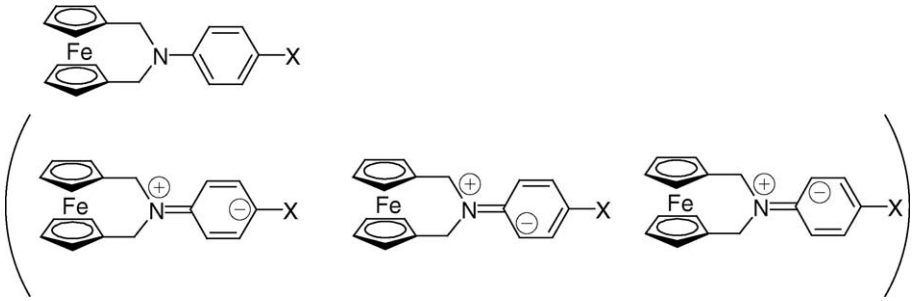

Scheme 2.

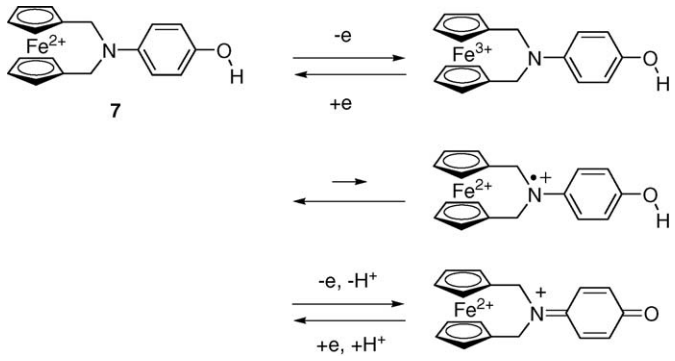

Scheme 3.

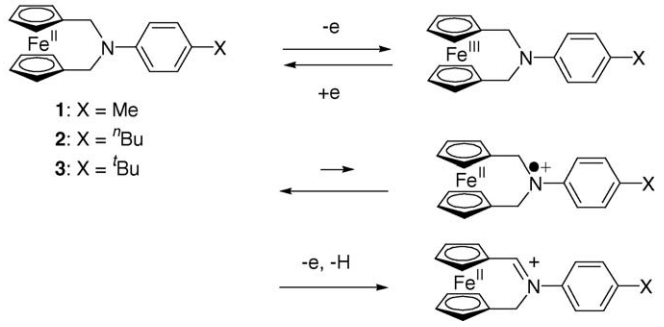

Scheme 4.

trochemical behaviors are explained by the mechanism shown in Scheme 4.

Higher potential of the second electrochemical oxidation of these compounds than that of **6** is ascribed to lower stability of the product of two electron oxidation than the oxidized species of **6**. Lack of reversibility also suggests that the oxidized product causes an irreversible chemical reaction such as abstraction of a hydrogen atom of the CH_2 group.

3. Electro- and photochemical behavior of azobenzene-containing ferrocenophanes

Since photo- and thermally induced *cis–trans* isomerization of azobenzene changes their structure, dipole moment, and absorption peak positions, the compounds having an azobenzene group have been investigated as the materials whose physical properties are regulated by light irradiation [6]. Combining ferrocene, showing the stable redox, and the azobenzene group in a molecule was reported to provide smart molecular materials with a dual stimulus-response character. Azoferrocene was found to undergo *cis–trans* isomerization of the azo group induced by irradiation of a single green light, and the reaction rates and equilibrium are controlled by valence of the Fe center [7]. Ferrocene derivative having azobenzene groups that bridge the cyclopentadienyl ligands was reported to change the molecular structure like a scissor by irradiation [8]. We applied the formation reaction of 2-aza[3]ferrocenophanes to preparation of the derivative having azobenzene group in the ligand. Coupling of 4-aminoazobenzene with ferrocenophanes **4** and **5** having a bromophenyl group at the nitrogen atom promoted by Pd(II) complexes [9] forms the compounds with the azobenzene groups **21** and **22**, as shown in Scheme 5 [10].

X-ray crystallography of **21** and **22** indicates *trans*-azobenzene group. These compounds have π–π^* absorption in visible region (λ_{max} = 442 and 426 nm, respectively), which are higher than that of 4-aminoazobenzene (λ_{max} = 390 nm) due to the electron donating azaferrocenophane group attached to the azobenzene group [11]. Irradiation of **21** and **22** at 420 nm causes decrease of the peaks, suggesting isomerization of the azobenzene group to *cis* form. Positions of the peaks due to n–π^* absorption of *cis*-azobenzene group were not determined in the original spectra due to a small intensity of the peak and its overlap with the peak of *trans*-azobenzene group existing in a solution under the photostationary state. Fig. 1 shows difference spectrum of **22** before and after irradiation which indicates growth of a small peak at 522 nm due to n–π^* absorption of the

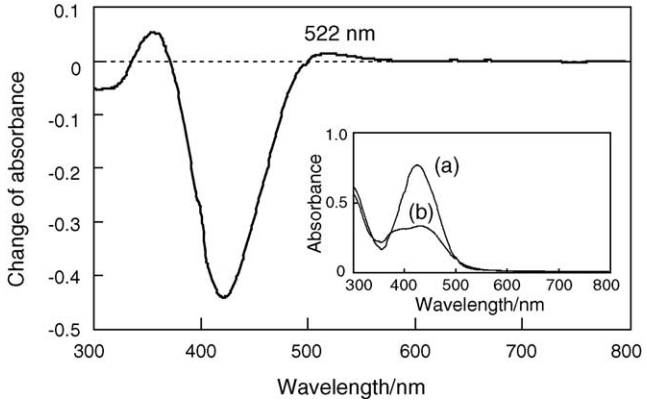

Fig. 1. Difference absorption spectrum of **22** after and before irradiation at 420 nm. The original spectra are in inset: (a) before irradiation and (b) after irradiation.

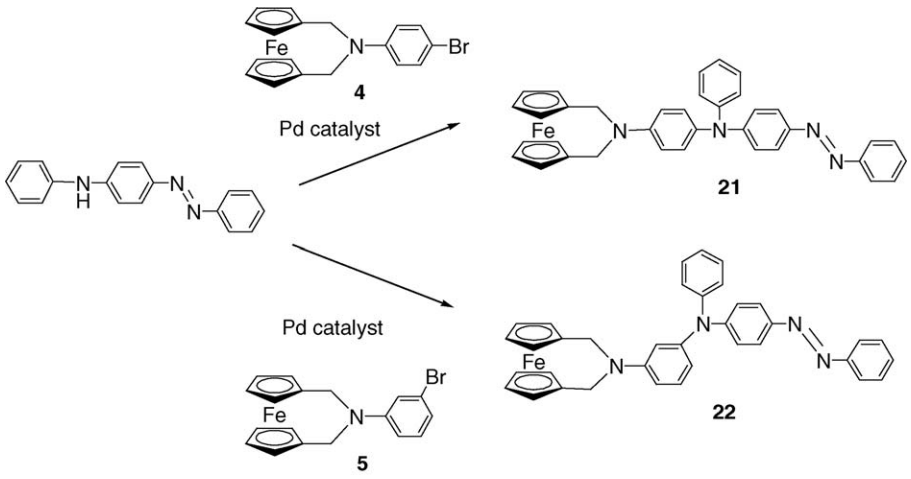

Scheme 5.

cis-azobenzene group. The corresponding peak of **21** is observed at 563 nm.

The *cis*-azobenzene group formed under photostationary state undergoes thermal isomerization to regenerate the compound with *trans*-azobenzene group in solution.

Compounds **21** and **22** undergo multi-step electrochemical oxidation and reduction. Fig. 2 shows the cyclic voltammogram of the compounds.

Three cycles of reversible electrochemical oxidation and reduction are observed for **21**, while **22** exhibits reversible redox between the Fe(II) and Fe(III) centers and one quasi-reversible electrochemical oxidation. Scheme 6 depicts the plausible mechanism of these electrochemical reactions of **21**. Second oxidation at $E_{1/2} = 0.41$ V converts an equilibrium mixture of ferrocenium and ferrocene with the ligand having radical cation into the Fe(II) species with dicationic diazaquinoid ligand. Positive charge in the ligand is stabilized by the π-conjugated group. The third reversible electrochemical reaction is assigned to redox of the Fe center having the dicationic ligand.

Second oxidation of **22** occurs at a much higher potential than the corresponding reaction of **21** due to lack of such a stabilized structure in the oxidized species of **22**. It partly induces concurrent hydrogen abstraction from the CH_2 group of the ligand.

Electrochemical oxidation of **21** under photostationary state at 0.30 V results in significant enhancement of the thermally induced isomerization of the *cis*- to *trans*-azobenzene group. Table 2 summarizes kinetic data for the isomerization before and after electrochemical oxidation. The reaction without applying electrochemical potential proceeds with $k_{obs} = 1.5 \times 10^{-3}\ s^{-1}$ at 283 K, whereas it increases to $6.3 \times 10^{-3}\ s^{-1}$ after oxidation at 0.30 V. Compound **22** shows more significant increase of the rate constant ($1.0 \times 10^{-4}\ s^{-1}$ before oxidation and $1.0 \times 10^{-2}\ s^{-1}$ after oxidation). Thus, the species formed by one electron oxidation of **22** with *cis*-azobenzene group undergoes thermal isomerization much more rapidly than unoxidized **22**. Scheme 7 illustrates a mechanism proposed for the isomerization of the oxidized species.

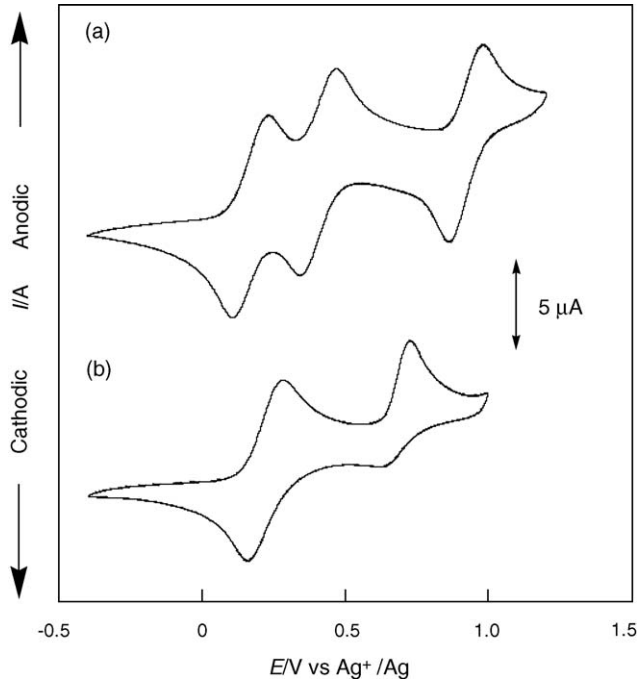

Fig. 2. Cyclic voltammograms in CH_2Cl_2 containing 0.10 M $^nBu_4NPF_6$ at 25 °C. Sweep rate, 0.10 V s^{-1}: (a) **21** (1.0 mM), $E_{1/2} = 0.17$, 0.41, and 0.92 V; (b) **22** (1.0 mM), $E_{1/2} = 0.22$ V and $E_{pa} = 0.73$ V.

Table 2
The rate constants for *cis–trans* thermal isomerization

Compound	E_{app}/V vs. Ag^+/Ag[a]	k_{obs} ($\times 10^3\ s^{-1}$) (283 K)[b]
21	Without oxidation	1.5
	0.30	6.3
	0.60	13.0
	1.0	19.0
22	Without oxidation	0.10
	0.4	10.0
	0.8	13.0

[a] Flow electrolysis at applied potentials, E_{app}, in toluene containing $^nBu_4NPF_6$ as an electrolyte.

[b] After photoirradiation in the 1 cm × 1 cm quartz cell at 420 nm from a cut-off filtered xenon lamp for 1 h at 20 °C.

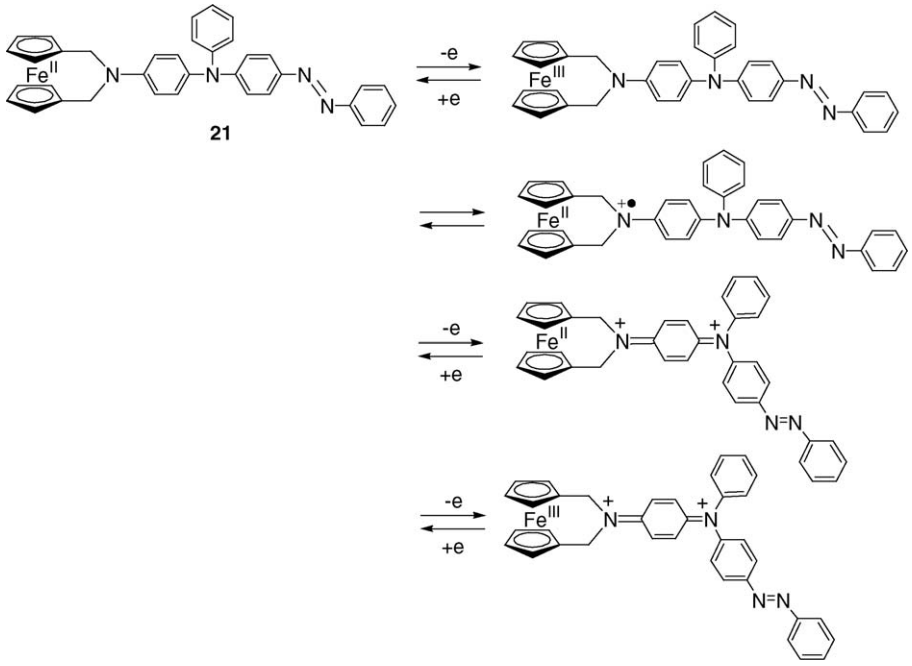

Scheme 6.

A species **A** contained in the solution after electrochemical oxidation has a radical cation at the nitrogen atom of the ferrocenophane fragment. Intramolecular electron transfer from the triarylamino group to the radical cation forms the isomer of the radical cation **B**. The compounds with a structure **B** has a canonical form containing azaquinodiimmine structure and radical cation at one nitrogen atom of the azo group. The N–N bond of this structure is expected to show a single bond character, which facilitates the isomerization of the *cis*-azobenzene group into the thermodynamically more stable *trans*-azobenzene via rotation of the bond between the nitrogen atoms.

Electrochemical and optical behavior of **22** is summarized in Scheme 8. In the unoxidized state with Fe(II) center and neutral ligand, the compound undergoes photo-isomerization by irradiation at 420 nm to reach the photostationary state. Thermally induced isomerization of the *cis*-azobenzene group formed by the irradiation takes place with moderate reaction rates.

Upon electrochemical oxidation, *cis*-azobenzene group of the compound, formed photochemically, undergoes the isomerization to the *trans*-azobenzene much more rapidly. The oxidation produces an equilibrium mixture containing the Fe(II) species with radical cation in the ligand, although it is expressed as the Fe(III) species in Scheme 8 for simplicity. Photoirradiation of

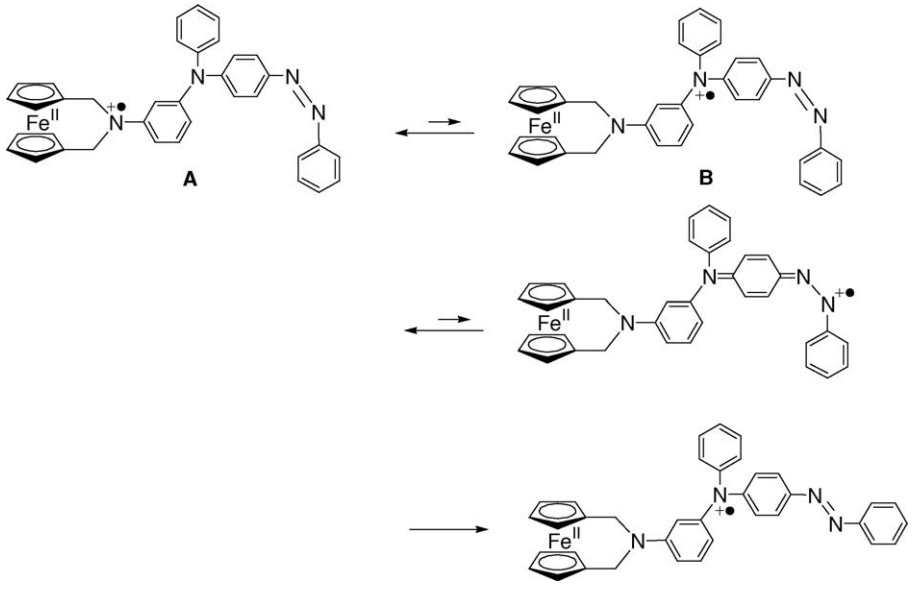

Scheme 7.

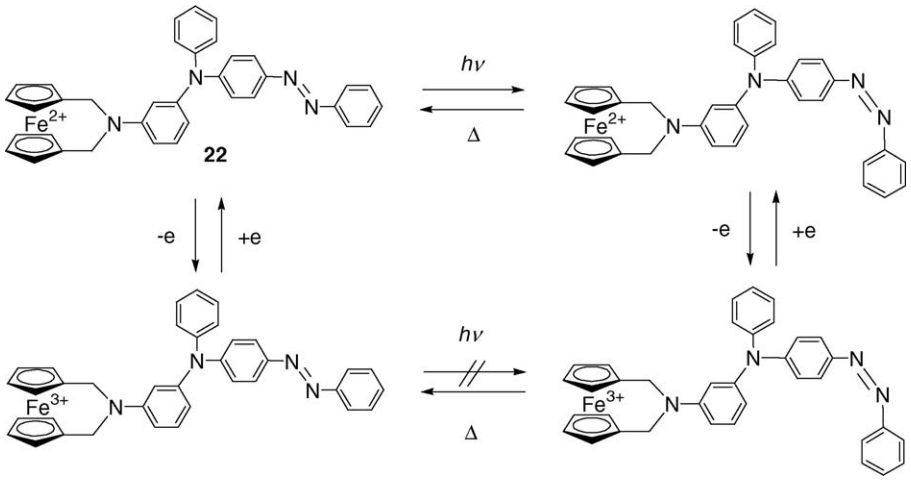

Scheme 8.

21 with a *trans*-azobenzene group after one electron oxidation causes the isomerization into the *trans*-azobenzene to almost negligible extent probably due to facile thermal isomerization of the *cis*-azobenzene group. Thus the photo-induced isomerization of the *trans*-azobenzene group is locked after one electron oxidation of the molecule, while it is released by electrochemical reduction to regenerate the neutral azaferrocenophane.

4. Formation of pseudorotaxane induced by electrochemical oxidation

Dialkylammonium was reported to be included in pore of crown ethers with suitable ring sizes [12]. The aminomethylcyclopentadienyl group of a ferrocene derivative is expected to undergo such complexation with a crown ether to form a pseudorotaxane having redox-active ferrocene unit in the vicinity of the ammonium complexed with crown ether [13,14]. Scheme 9 displays the results of preparation of dialkylammonium containing the ferrocene derivative and their formation of pseudorotaxane with dibenzo[24]crown-8 (DB24C8). Treatment of **23** and **24** with HCl_{aq} and NH_4PF_6 forms the ferrocene with dialkylammonium group of the ligand and PF_6^- counter anion, [**23**-H]$^+$(PF_6) and [**24**-H_2]$^{2+}$(PF_6)$_2$, as shown in Scheme 9.

The complexation of [**23**-H]$^+$(PF_6) and DB24C8 results in formation of [2]pseudorotaxane, [(DB24C8)(**23**-H)]$^+$(PF_6), composed of the ferrocene derivative with dialkylammonium group in the ligand. Analogous reaction of [**24**-H_2]$^{2+}$(PF_6)$_2$ yields [3]pseudorotaxane, [(DB24C8)$_2$(**24**-H_2)]$^{2+}$(PF_6)$_2$. The obtained pseudorotaxanes isolated as solids were characterized by X-ray crystallography and IR spectroscopy.

X-ray crystallography of the pseudorotaxanes revealed the interlocked structure composed of the dialkylammonium group of the ferrocene-containing molecule and DB24C8, as shown in Fig. 3.

The NH_2 and CH_2 groups of the axis of the former pseudorotaxane show short contacts with the oxygen atoms of DB24C8 (NH···O 2.18 Å and CH···O 2.35 Å) due to the N–H···O and C–H···O interaction between the axis and cyclic molecules. The aromatic planes of the axis and cyclic molecules are stacked to each other with a distance of the planes with 3.34 Å. Two DB24C8 molecules of [(DB24C8)$_2$(**24**-H_2)]$^{2+}$(PF_6)$_2$ include the cationic dialkylammonium groups of the dicationic axis molecule. IR spectrum of the pseudorotaxanes also exhibits the peaks characteristic for the interlocked structure. [(DB24C8)(**23**-H)]$^+$(PF_6) shows peaks due to asymmetric and symmetric vibration of the NH_2 group at 3166 and 3067 cm^{-1}, respectively. The peak positions are much lower than those of the peaks of the ionic compound without DB24C8,

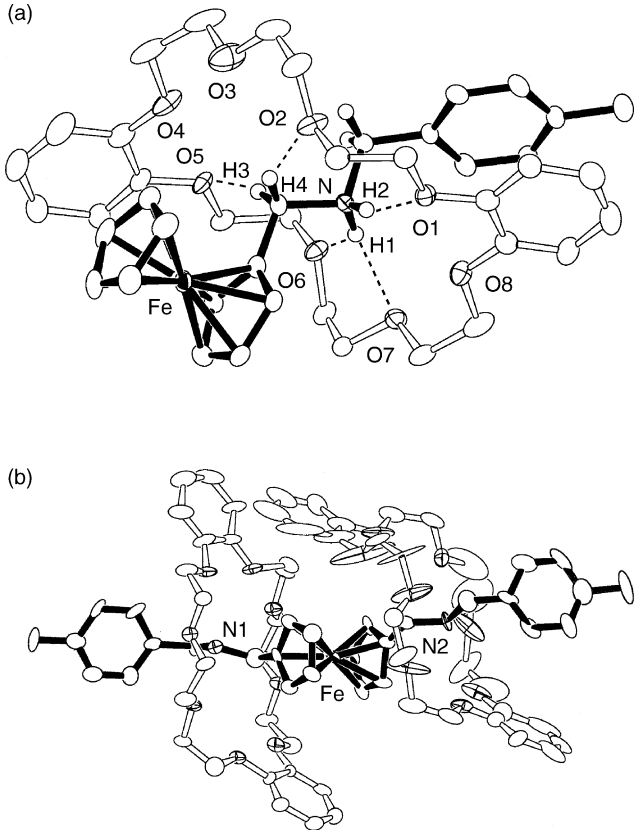

Fig. 3. Molecular structures of the pseudorotaxanes: (a) [(DB24C8)(**23**-H)]$^+$(PF_6) and (b) [(DB24C8)$_2$(**24**-H_2)]$^{2+}$(PF_6)$_2$.

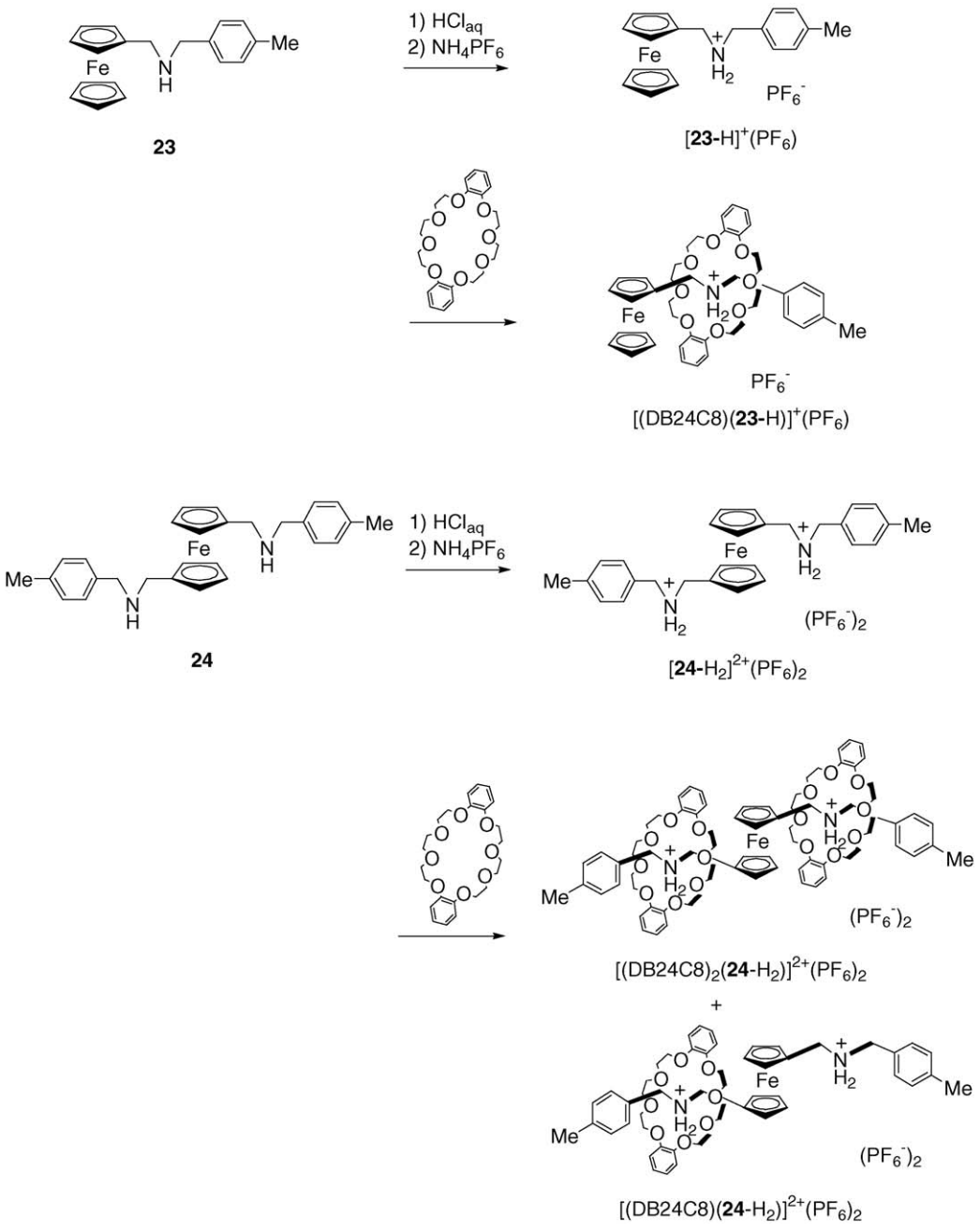

Scheme 9.

[**23**-H]$^+$(PF$_6$), which contains the ν_{as} and ν_s vibration peaks at 3266 and 3233 cm^{-1}.

The pseudorotaxane species were characterized by ^{1}H NMR and mass spectrometry, although the solution contains free ferrocene containing axis molecules and DB24C8 formed by equilibrium between these species. A mixture formed from equimolar [**23**-H]$^+$(PF$_6$) and DB24C8 in CD$_3$CN shows the ^{1}H NMR peaks of CH$_2$N hydrogens at 4.53, 4.37, 4.06, and 4.04 ppm. The two former signals are assigned to those of [(DB24C8)(**23**-H)]$^+$(PF$_6$), while the latter peaks are due to [**23**-H]$^+$(PF$_6$). The ratio of [**23**-H]$^+$(PF$_6$) to [(DB24C8)(**23**-H)]$^+$(PF$_6$) is determined as 49:51 from the peak intensity of the cyclopentadienyl hydrogens. More simple pseudorotaxane [(DB24C8)(PhCH$_2$NH$_2$CH$_2$Ph)]$^+$(PF$_6$) was also reported to show similar low filed shift of the CH$_2$N signals of the axis molecule caused by complexation with DB24C8 [12]. Mass spectrometry of the solution shows a peak at $m/z = 768$ which is assigned to the cationic part of [(DB24C8)(**23**-H)]$^+$(PF$_6$).

Pseudorotaxane of protonated species of **24** contains a more complicated mixture. A solution prepared by mixing [**24**-H$_2$]$^{2+}$(PF$_6$)$_2$ and DB24C8 in CD$_3$CN shows the ^{1}H NMR exhibits the signals of the CH$_2$–N hydrogens at 4.48 and 4.21 ppm due to [3]pseudorotaxane, [(DB24C8)$_2$(**24**-H$_2$)]$^{2+}$(PF$_6$)$_2$, and the signals at 4.56 and 4.38 ppm due to [2]pseudorotaxane, [(DB24C8)(**24**-H$_2$)]$^{2+}$(PF$_6$)$_2$. Signals of the axis molecule without the macrocycle, [**24**-H$_2$]$^{2+}$(PF$_6$)$_2$, con-

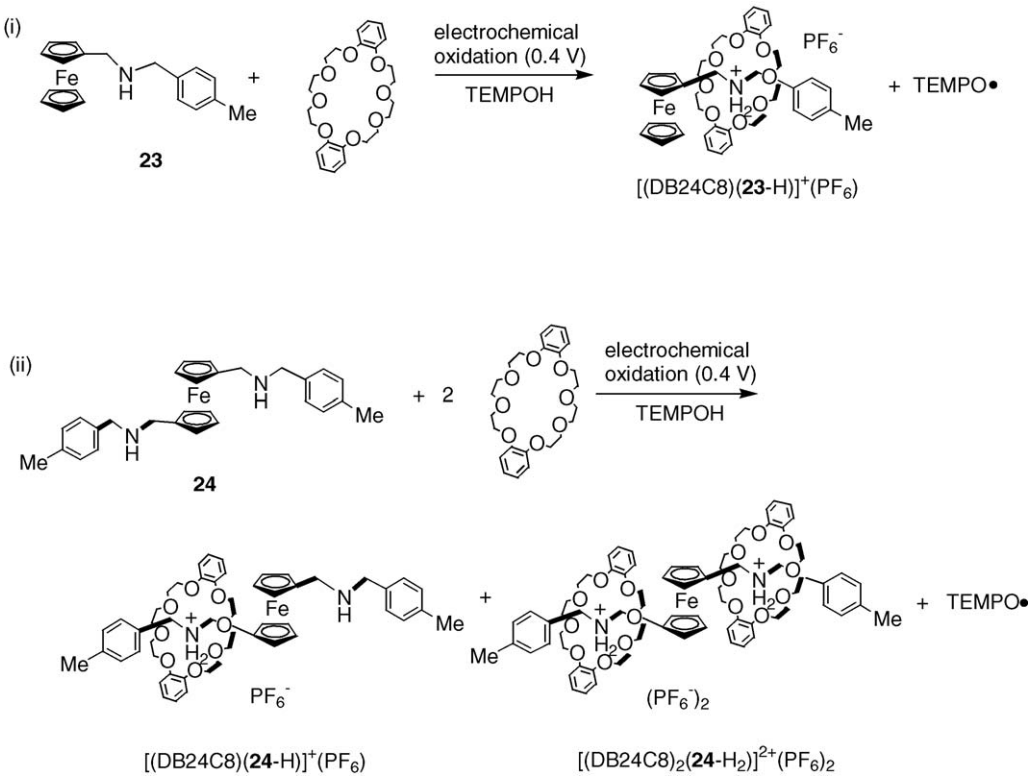

Scheme 10.

tained in the solution are also observed. These results in addition to the mass spectra of the solution indicate that the axis, [2]pseudorotaxane, and [3]pseudorotaxane are contained in the solution and that they are in equilibrium by inclusion of the dialkylammonium groups by DB24C8 and their dissociation.

The pseudorotaxanes shown above are formed from an independent reaction that involves electrochemical oxidation of the **23** (or **24**) in the presence of a source of hydrogen radical and DB24C8, as described in Scheme 10.

Electrochemical oxidation of **23** and **24** at 0.4 V (versus Ag^+/Ag) in the presence of DB24C8 and 1-hydroxy-2,2,6,6-tetramethylpiperidine (TEMPOH) produces the pseudorotaxanes composed of the ferrocene derivatives with the dialkylammonium group and DB24C8. A mixture of the [2] and [3]pseudorotaxanes, $[(DB24C8)(\mathbf{24}\text{-}H)]^+$ and $[(DB24C8)_2(\mathbf{24}\text{-}H_2)]^{2+}$ is obtained from the oxidation of **24** at the same potential in the presence of TEMPOH and DB24C8. Formation of the pseudorotaxanes was confirmed by FABMS spectra of the solutions by using flow electrolysis technique [15], shown in Fig. 4.

A minimum volume of the cell for electrolysis enables characterization of the species formed by electrochemical reactions by spectroscopies. Flow electrolysis of **23** in the presence of TEMPOH and DB24C8 at 0.4 V leads to the formation of $[(DB24C8)(\mathbf{23}\text{-}H)]^+$ which shows a peak at $m/z = 748$ in the mass spectrum. The CH_3CN solution after flow electrolysis of **24** in the presence of TEMPOH and DB24C8 at 0.4 V shows the FAB mass peak at $m/z = 674$ corresponding to the dicationic [3]pseudorotaxane, $[(DB24C8)_2(\mathbf{24}\text{-}H_2)]^{2+}$ and that at $m/z = 901$ due to the monocationic [2]pseudorotaxane, $[(DB24C8)(\mathbf{24}\text{-}H)]^+$. These reactions convert TEMPOH quantitatively into TEMPO radical which was identified by characteristic ESR signal.

Formation of the pseudorotaxanes indicates that the electrochemical oxidation in the presence of TEMPOH induces formal protonation of the dialkylamine group affording the ferrocene derivatives with the dialkylammonium group of the ligands. In order to clarify details of the reaction, we investigated the reaction without TEMPOH and/or without DB24C8. Scheme 11 depicts the reaction mechanism proposed based on the experimental results of **23**.

Electrochemical oxidation of **23** produces ferrocenium species **A** which is equilibrated with the species having radical cation at the nitrogen atom **B** in the solution. The radical cation formed partly in the solution reacts with TEMPOH to form the

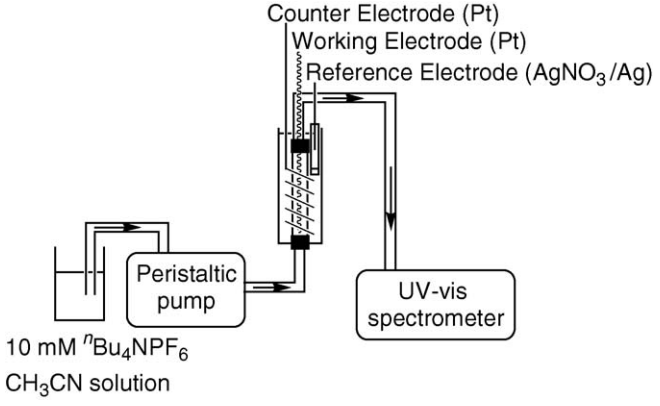

Fig. 4. Schematic diagram of the flow electrolysis system.

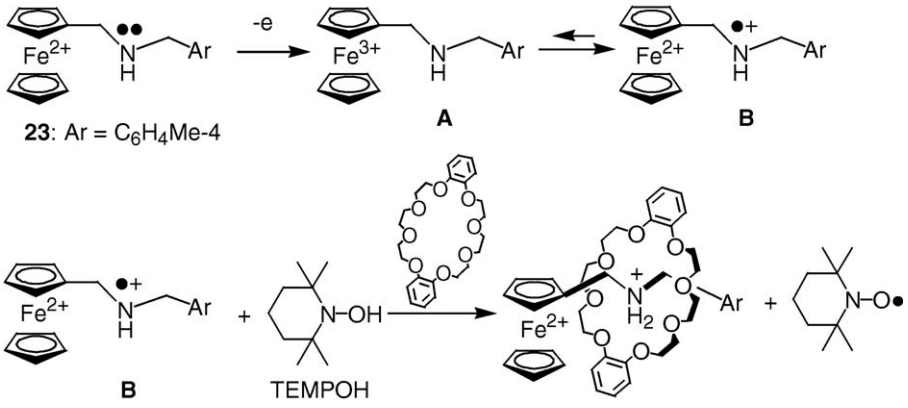

Scheme 11.

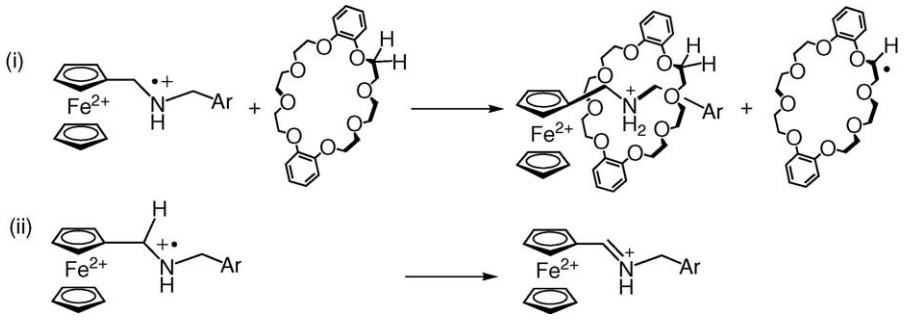

Scheme 12.

dialkylammonium via abstraction of the hydrogen atom from TEMPOH. The formed cationic species forms the pseudorotaxane. This mechanism was supported by experimental results shown below.

Cyclic voltammogram (CV) and linear sweep voltammogram during the electrochemical oxidation of **23** indicate that the quantitative one electron oxidation at 0.40 V (versus Ag^+/Ag) converts the ferrocenylene group into ferrocenium in >98%. The absorption spectra of the solution during the electrochemical oxidation without addition of TEMPOH show immediate formation of a peak at 630 nm and its gradual decrease. Addition of TEMPOH to the solution causes rapid disappearance of the peak due to the abstraction of a hydrogen atom from TEMPOH. Addition of DB24C8 to the solution or keeping it at room temperature causes gradual decrease of the peak due to ferrocenium, indicating that the formation of dialkylammonium via hydrogen abstraction occurs under these conditions also. Detailed kinetic measurement revealed the following points. The reaction rates increase with increase of concentration of DB24C8, although it is much slower than the reaction in the presence of TEMPOH. In the absence of the additives, decrease of the ferrocenium takes place but in a much slower rate than the reaction in the presence of DB24C8. Scheme 12 depicts the mechanism of formation of the cationic species in the presence and absence of DB24C8.

DB24C8 in the reaction (i) has dual roles. It donates hydrogen atom to the radical action of the ferrocene-containing axis molecule. On the other hand, it includes the dialkylammonium formed by the reaction in the pore. Since the mass spectroscopy indicates the peaks corresponding to the pseudorotaxane containing DB24C8, it binds the cationic axis molecule more firmly than the cyclic compound which loses a hydrogen atom and possibly another hydrogen atom to form the unsaturated compound. Use of a smaller crown ether which does not allow inclusion of such axis molecule also forms the dialkylammonium, indicating that the inclusion of the axis molecule by DB24C8 is not preceded by the inclusion by the macrocycle.

In summary, we obtained new ferrocene derivatives whose cyclopentadienyl ligands are functionalized by amino groups. Electronic communication between the Fe center and the nitrogen atom at the oxidized states enabled regulation of *cis–trans* isomerization of the azobenzene group of the ligand and rotaxane formation induced by electrochemical oxidation.

Acknowledgments

This work was financially supported by Grants-in-aid for Scientific Research from the Ministry of Education, Culture, Sport, Science, and Technology, Japan, and by Shorai Foundation from Harima Kasei Co. Ltd.

References

[1] (a) A. Togni, T. Hayashi (Eds.), Ferrocenes, VCH, New York, 1995;
(b) P. Nguyen, P. Gomez-Elipe, I. Manners, Chem. Rev. 99 (1999) 1515;

(c) T.J. Colacot, Chem. Rev. 103 (2003) 3101, and references cited therein.
[2] H. Plenio, J. Yang, R. Diodone, J. Heinze, Inorg. Chem. 33 (1994) 4098.
[3] (a) S.-I. Murahashi, K. Kondo, T. Hakata, Tetrahedron Lett. 23 (1982) 229;
(b) Y. Watanabe, Y. Tsuji, H. Ige, Y. Ohsugi, T. Ohta, J. Org. Chem. 49 (1984) 3359;
(c) Y. Tsuji, K.-T. Huh, Y. Ohsugi, Y. Watanabe, J. Org. Chem. 50 (1985) 1365;
(d) Y. Tsuji, K.-T. Huh, Y. Yokoyama, Y. Watanabe, J. Chem. Soc., Chem. Commun. (1986) 1575;
(e) Y. Tsuji, Y. Yokoyama, K.-T. Huh, Y. Watanabe, Bull. Chem. Soc. Jpn. 60 (1987) 3456.
[4] (a) I. Yamaguchi, K. Osakada, T. Yamamoto, J. Am. Chem. Soc. 118 (1996) 1811;
(b) I. Yamaguchi, K. Osakada, T. Yamamoto, Macromolecules 30 (1997) 4288;
(c) I. Yamaguchi, K. Osakada, T. Yamamoto, Polym. Bull. 42 (1999) 141.
[5] (a) I. Yamaguchi, T. Sakano, H. Ishii, K. Osakada, T. Yamamoto, J. Organometall. Chem. 584 (1999) 213;
(b) T. Sakano, H. Ishii, I. Yamaguchi, K. Osakada, T. Yamamoto, Inorg. Chim. Acta 296 (1999) 176;
(c) T. Sakano, M. Horie, K. Osakada, H. Nakao, Bull. Chem. Soc. Jpn. 74 (2001) 2059.
[6] (a) K. Ichimura, Chem. Rev. 100 (2000) 1847;
(b) N. Tamai, H. Miyasaka, Chem. Rev. 100 (2000) 1875;
(c) I. Yamaguchi, K. Osakada, T. Yamamoto, Chem. Commun. (2000) 1335;
(d) T. Ikeda, J. Mater. Chem. 13 (2003) 2037.
[7] (a) M. Kurihara, T. Matsuda, A. Hirooka, T. Yutaka, H. Nishihara, J. Am. Chem. Soc. 122 (2000) 12373;
(b) M. Kurihara, A. Hirooka, S. Kume, M. Sugimoto, H. Nishihara, J. Am. Chem. Soc. 124 (2002) 8800;
(c) A. Sakamoto, A. Hirooka, K. Namiki, M. Kurihara, M. Murata, M. Sugimoto, H. Nishihara, Inorg. Chem. 44 (2005) 7547.
[8] T. Muraoka, K. Kinbara, Y. Kobayashi, T. Aida, J. Am. Chem. Soc. 125 (2003) 5612.
[9] (a) J.F. Hartwig, S. Richards, D. Barañano, F. Paul, J. Am. Chem. Soc. 118 (1996) 3626;
(b) J.F. Hartwig, Synlett (1997) 329;
(c) M.S. Driver, J.F. Hartwig, J. Am. Chem. Soc. 119 (1997) 8232;
(d) L.M. Alcazar-Roman, J.F. Hartwig, A.L. Rheingold, L.M. Liable-Sands, I.A. Guzei, J. Am. Chem. Soc. 122 (2000) 4618;
(e) A.S. Guram, R.A. Rennels, S.L. Buchwald, Angew. Chem., Int. Ed. Engl. 34 (1995) 1348;
(f) J.P. Wolfe, S. Wagaw, S.L. Buchwald, J. Am. Chem. Soc. 118 (1996) 7215;
(g) S. Wagaw, R.A. Rennels, S.L. Buchwald, J. Am. Chem. Soc. 119 (1997) 8451;
(h) J.-F. Marcoux, S. Wagaw, S.L. Buchwald, J. Org. Chem. 62 (1997) 1568;
(i) R.A. Singer, J.P. Sadighi, S.L. Buchwald, J. Am. Chem. Soc. 120 (1998) 213;
(j) D.W. Old, M.C. Harris, S.L. Buchwald, Org. Lett. 2 (2000) 1403;
(k) N.P. Reddy, M. Tanaka, Tetrahedron Lett. 38 (1997) 4807;
(l) M. Nishiyama, T. Yamamoto, Y. Koie, Tetrahedron Lett. 39 (1998) 617;
(m) T. Yamamoto, M. Nishiyama, Y. Koie, Tetrahedron Lett. 39 (1998) 2367.
[10] (a) M. Horie, T. Sakano, K. Osakada, H. Nakao, Organometallics 23 (2004) 18;
(b) T. Sakano, M. Horie, K. Osakada, H. Nakao, Eur. J. Inorg. Chem. (2005) 644.
[11] Y. Hirose, H. Yui, T. Sawada, J. Phys. Chem. A 106 (2002) 3067.
[12] (a) P.R. Ashton, P.J. Campbell, E.J.T. Chrystal, P.T. Glinke, S. Menzer, D. Philp, N. Spencer, J.F. Stoddart, P.A. Tasker, D.J. Williams, Angew. Chem., Int. Ed. Engl. 34 (1995) 1865;
(b) A.G. Kolchinski, D.H. Busch, N.W. Alcock, J. Chem. Soc., Chem. Commun. (1995) 1289;
(c) F.M. Raymo, J.F. Stoddart, Chem. Rev. 99 (1999) 1643;
(d) V. Balzani, A. Credi, F.M. Raymo, J.F. Stoddart, Angew. Chem. Int. Ed. 39 (2000) 3348;
(e) V. Balzani, M. Venturi, A. Credi, Molecular Devices and Machines—A Journey into the Nanoworld, Wiley/VCH, Weinheim, 2003.
[13] (a) M. Horie, Y. Suzaki, K. Osakada, J. Am. Chem. Soc. 126 (2004) 3684;
(b) M. Horie, Y. Suzaki, K. Osakada, Inorg. Chem. 44 (2005) 5844.
[14] N. Kihara, M. Hashimoto, T. Takata, Org. Lett. 6 (2004) 1693.
[15] H. Nakao, H. Hayashi, K. Okita, Anal. Sci. 17 (2001) 545.